J|A|C|S ARTICLES

Published on Web 02/17/2010

Diastereoisomerically Pure Fulleropyrrolidines as Chiral Platforms for the Design of Optically Active Liquid Crystals

Stéphane Campidelli,[†,⊥] Philippe Bourgun,[†] Boris Guintchin,[†] Julien Furrer,[‡] Helen Stoeckli-Evans,[§] Isabel M. Saez,[||] John W. Goodby,*[,||] and Robert Deschenaux*[,†]

Institut de Chimie, Université de Neuchâtel, Avenue de Bellevaux 51, Case Postale 158, 2009 Neuchâtel, Switzerland, Service Analytique Facultaire, Institut de Chimie, Université de Neuchâtel, Avenue de Bellevaux 51, 2009 Neuchâtel, Switzerland, Institut de Physique, Université de Neuchâtel, Rue Emile-Argand 11, 2009 Neuchâtel, Switzerland, and Department of Chemistry, The University of York, Heslington, York YO10 5DD, U.K.

Received December 2, 2009; E-mail: jwg500@york.ac.uk; robert.deschenaux@unine.ch

Abstract: Incorporation of [60]fullerene (C_{60}) within self-organizing systems is conceptually challenging but allows us to obtain materials which combine the characteristics (anisotropy, organization) of condensed mesophases with the properties of C_{60} (photo- and electrochemical activity). Here, we report on the synthesis, characterization, and liquid-crystalline properties of four optically active fullerodendrimers, which are chiral at the point of conjunction between the fullerene scaffold and the mesogenic moieties. Thus, the novelty of this study is to take advantage of the asymmetric carbon atom created during the 1,3-dipolar cycloaddition reaction on C_{60} in order to induce mesoscopic chirality in the materials. Four diastereoisomeric fulleropyrrolidines ((*R*,*S*)-**1**, (*R*,*R*)-**1**, (*S*,*R*)-**1**, and (*S*,*S*)-**1**) were synthesized and associated with a second-generation nematic (N) dendron to give fullerodendrimers ((*R*,*S*)-**2**, (*R*,*R*)-**2**, (*S*,*R*)-**2**, and (*S*,*S*)-**2**) which display chiral nematic (N*) phases. The absolute configurations of the stereogenic centers were determined by X-ray crystallography, 1D and 2D NMR experiments, and circular dichroism (CD) spectroscopy. The liquid-crystalline properties of the fullerodendrimers were studied by polarized optical microscopy (POM) and differential scanning calorimetry (DSC). The fulleropyrrolidine derivatives **2** exhibit supramolecular helicoidal organizations with a right-handed helix for the (*R*,*S*)-**2** and (*R*,*R*)-**2** diastereoisomers and a left-handed helix for the (*S*,*R*)-**2** and (*S*,*S*)-**2** diastereoisomers. This result suggests that the self-organization of such supermolecular materials can be controlled at the molecular level by the introduction of only one chiral center.

Introduction

With the successful development of the nanotechnologies via a bottom-up approach, the design of self-organizing nanostructures obtained by the organization of multifunctional molecular units has attracted much attention in the scientific community.[1,2] In this context, liquid crystals are important systems, as their self-organization can be controlled in order to generate complex supramolecular architectures, the properties of which can be tuned by structural engineering at the molecular level.[3] Chiral nematic (N*) and chiral smectic C (SmC*) phases and their attendant physical properties such as thermochromism, ferroelectricity, and pyroelectricity have found numerous practical applications in, for example, displays, light modulators, and thermal imaging devices. The presence of [60]fullerene (C_{60}) in such mesophases opens opportunities for the design of liquid crystals displaying novel electro- and photoactive properties within a designed/desirable chiral supramolecular environment.

The functionalization of C_{60} with mesomorphic malonates (via the Bingel reaction[4]) or with mesomorphic aldehydes (via the 1,3-dipolar cycloaddition reaction[5,6]) has led to liquid-crystalline methanofullerenes or fulleropyrrolidines, respectively, which display smectic,[7−9] columnar,[10−12] ne-

[†] Institut de Chimie, Université de Neuchâtel.
[‡] Service Analytique Facultaire, Université de Neuchâtel.
[§] Institut de Physique, Université de Neuchâtel.
[||] University of York.
[⊥] Current address: CEA, IRAMIS, Laboratoire d'Electronique Moléculaire, 91191 Gif sur Yvette, France.

(1) Huck, W. T. S. *Nanoscale Assembly*; Springer: New York, 2005.
(2) Schlüter, A. D. *Functional Molecular Nanostructures*; Springer: New York, 2005.
(3) (a) Kato, T.; Mizoshita, N.; Kishimoto, K. *Angew. Chem., Int. Ed.* **2006**, *45*, 38. (b) Saez, I. M.; Goodby, J. W. *Struct. Bonding (Berlin)* **2008**, *128*, 1.
(4) Bingel, C. *Chem. Ber.* **1993**, *126*, 1957.
(5) Confalone, P. N.; Huie, E. M. *J. Org. Chem.* **1983**, *48*, 2994.
(6) (a) Prato, M.; Maggini, M. *Acc. Chem. Res.* **1998**, *31*, 519. (b) Tagmatarchis, N.; Prato, M. *Synlett* **2003**, *6*, 768.
(7) (a) Dardel, B.; Guillon, D.; Heinrich, B.; Deschenaux, R. *J. Mater. Chem.* **2001**, *11*, 2814. (b) Campidelli, S.; Vázquez, E.; Milic, D.; Prato, M.; Barberá, J.; Guldi, D. M.; Marcaccio, M.; Paolucci, D.; Paolucci, F.; Deschenaux, R. *J. Mater. Chem.* **2004**, *14*, 1266. (c) Allard, E.; Oswald, F.; Donnio, B.; Guillon, D.; Delgado, J. L.; Langa, F.; Deschenaux, R. *Org. Lett.* **2005**, *7*, 383. (d) Campidelli, S.; Lenoble, J.; Barberá, J.; Paolucci, F.; Marcaccio, M.; Paolucci, D.; Deschenaux, R. *Macromolecules* **2005**, *38*, 7915. (e) Campidelli, S.; Pérez, L.; Rodrígez-López, J.; Barberá, J.; Langa, F.; Deschenaux, R. *Tetrahedron* **2006**, *62*, 2115.
(8) Felder-Flesch, D.; Rupnicki, L.; Bourgogne, C.; Donnio, B.; Guillon, D. *J. Mater. Chem.* **2006**, *16*, 304.
(9) Nakanishi, T.; Shen, Y.; Wang, J.; Yagai, S.; Funahashi, M.; Kato, T.; Fernandes, P.; Möhwald, H.; Kurth, D. G. *J. Am. Chem. Soc.* **2008**, *130*, 9236.

 10.1021/ja910128e

Scheme 1[a]

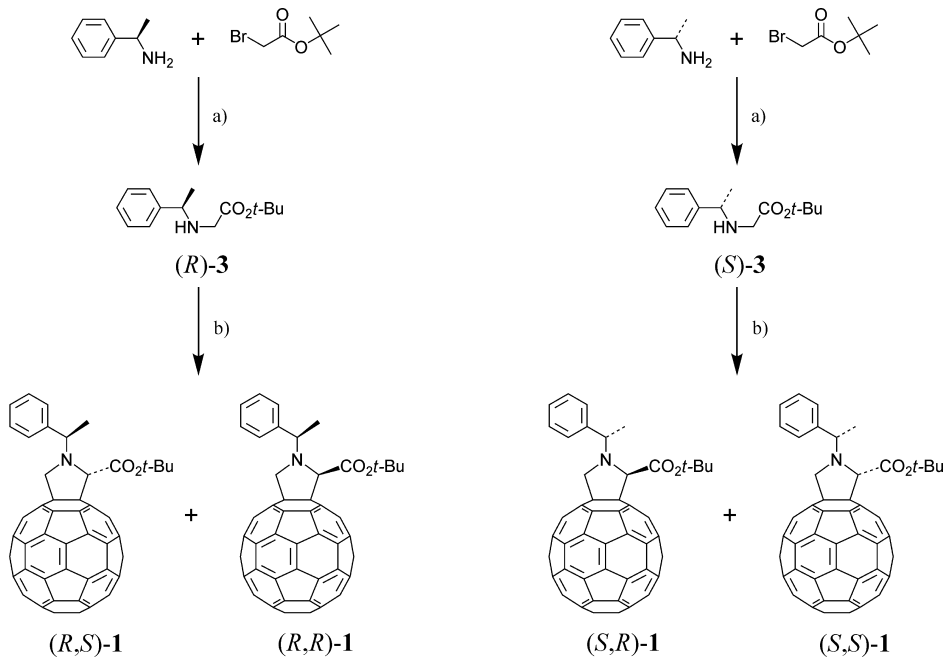

[a] Legend: (a) Et_3N, THF, 0 °C and then room temperature, overnight, 65% for (*R*)-**3**, 63% for (*S*)-**3**; (b) C_{60}, formaldehyde, toluene, reflux, 20 h, 26% for (*R*,*S*)-**1**, 15% for (*R*,*R*)-**1**, 25% for (*S*,*R*)-**1**, 22% for (*S*,*S*)-**1**.

matic,[7a,13] and chiral nematic[14] phases. Our concept, the use of dendrimers and dendrons[7,11] (prepared by convergent syntheses[15]) as mesomorphic promoters to functionalize C_{60}, is a successful approach because the nature and size of the dendrons can be modified to tailor the liquid-crystalline properties of the fullerene derivatives. It is worth noting that theoretical[16] and experimental studies[7,11] are in good agreement to explain the supramolecular organizations of fullerene-based molecular units within lamellar or columnar phases. The design of the above-mentioned chiral fullerodendrimers (N* phase) requires the synthesis of optically active dendrons, the purification of which can be demanding. Therefore, only second-generation dendrons could be prepared in reasonable yields and quantities.[17]

During the formation of fulleropyrrolidines by 1,3-dipolar cycloaddition, a stereogenic center in the pyrrolidine ring is generated when functionalized aldehydes (RCHO with R ≠ H) and amino acids are used.[6] For example, Prato et al. applied this reaction to the preparation of chiral fulleroprolines,[18] the absolute configurations of which were determined on the basis of experimental and calculated circular dichroism (CD) spectra. Other examples of chiral fulleropyrrolidines obtained by diastereo- and enantioselective syntheses have been reported.[19]

The aforementioned liquid-crystalline fulleropyrrolidines were obtained as racemic mixtures, since the reactions were carried out under standard conditions[6] without chiral reagents. We postulated that if optically active fulleropyrrolidines could be prepared, they would represent an interesting chiral platform for the design of optically active liquid crystals derived from nonchiral mesomorphic promoters. In this case, the fulleropyrrolidine and dendritic addend would play complementary roles: i.e., the dendron would generate mesophases (e.g., N, SmC) and the fulleropyrrolidine would make the mesophases chiral (i.e., N → N*, SmC → SmC*).

We describe herein the synthesis and liquid-crystalline and optical properties of four diastereoisomeric fullerodendrimers. A second-generation dendron which carries laterally branched mesogens was selected in order to observe the N* phase for the chiral fullerodendrimers. The stereochemistry for one diastereoisomer was determined by means of X-ray diffraction. From this result, the absolute configuration of the chiral centers of all of the diastereoisomers was established.

Results and Discussion

Design. This study is based on the association of diastereomerically pure fulleropyrrolidines ((*R*,*S*)-**1**, (*R*,*R*)-**1**, (*S*,*R*)-**1** and (*S*,*S*)-**1**) (Scheme 1), used as sources of chirality, with a second-generation dendron (**9**) (Scheme 2) which carries laterally branched mesogens. Thus, nematic behavior was expected from this dendritic system. Therefore, the optically active fullerodendrimers (Scheme 3) were expected to display the chiral nematic, N*, phase.

Synthesis. The four diastereoisomeric fulleropyrrolidines (*R*,*S*)-**1**, (*R*,*R*)-**1**, (*S*,*R*)-**1**, and (*S*,*S*)-**1** were synthesized by the addition of the *tert*-butyl ester protected amino acid (*R*)-**3** or (*S*)-**3** with formaldehyde to C_{60} under standard 1,3-dipolar addition conditions[6] (Scheme 1). Compounds (*R*)-**3** and (*S*)-**3** were prepared by reacting commercially available (*R*)-(+)- or (*S*)-(−)-α-methylbenzylamine with *tert*-butyl bromoacetate. The mixtures of diastereoisomers, (*R*,*S*)-**1**/(*R*,*R*)-**1** and (*S*,*R*)-**1**/(*S*,*S*)-**1**, were separated by column chromatography. In their respective syntheses, the (*R*,*S*)-**1** and (*S*,*R*)-**1** compounds eluted first. For

(10) Bushby, R. J.; Hamley, I. W.; Liu, Q.; Lozman, O. R.; Lydon, J. E. *J. Mater. Chem.* **2005**, *15*, 4429.
(11) (a) Lenoble, J.; Maringa, N.; Campidelli, S.; Donnio, B.; Guillon, D.; Deschenaux, R. *Org. Lett.* **2006**, *8*, 1851. (b) Lenoble, J.; Campidelli, S.; Maringa, N.; Donnio, B.; Guillon, D.; Yevlampieva, N.; Deschenaux, R. *J. Am. Chem. Soc.* **2007**, *129*, 9941.
(12) De la Escosura, A.; Martínez-Díaz, M. V.; Barberá, J.; Torres, T. *J. Org. Chem.* **2008**, *73*, 1475.
(13) (a) Tirelli, N.; Cardullo, F.; Habicher, T.; Suter, U. W.; Diederich, F. *J. Chem. Soc., Perkin Trans. 2* **2000**, 193. (b) Mamlouk, H.; Heinrich, B.; Bourgogne, C.; Donnio, B.; Guillon, D.; Felder-Flesch, D. *J. Mater. Chem.* **2007**, *17*, 2199.

Scheme 2[a]

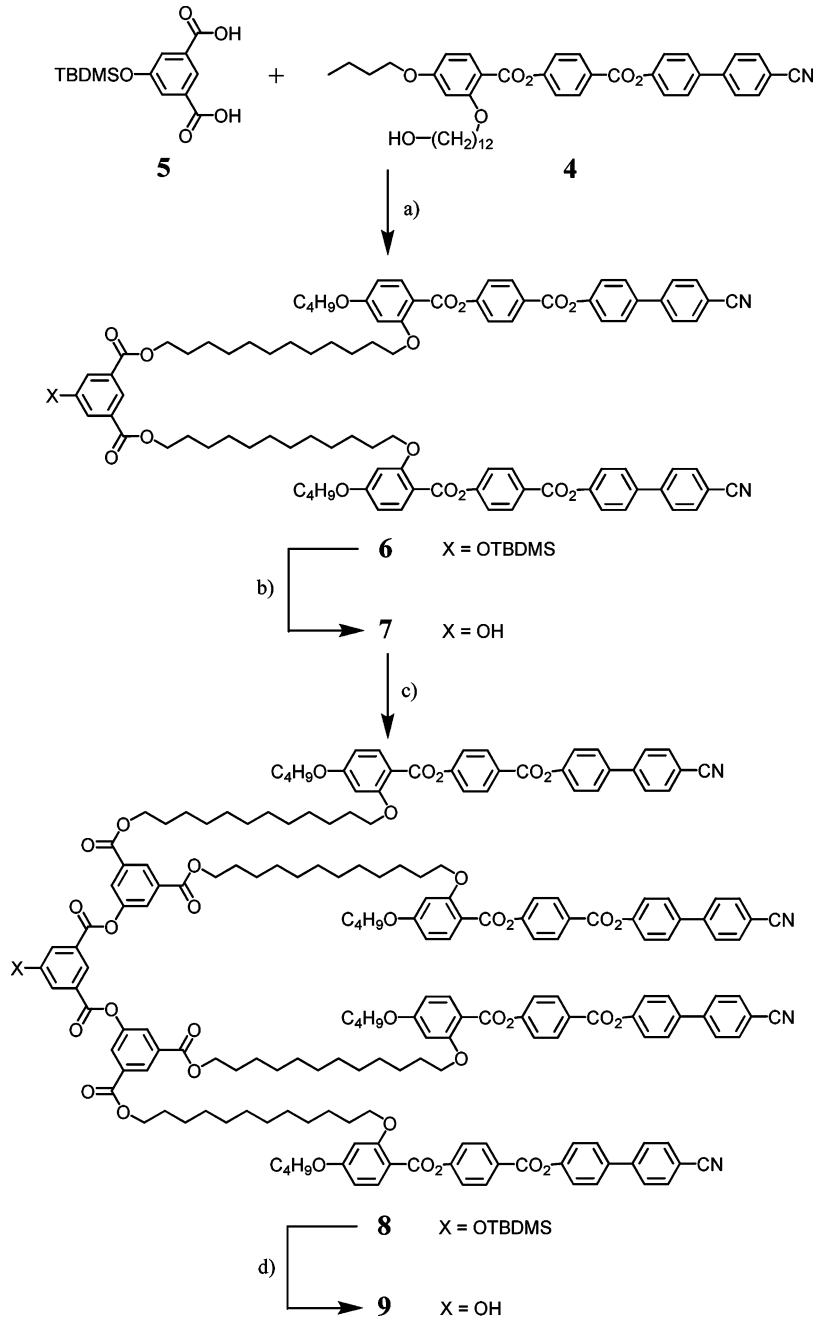

[a] Legend: (a) *N,N′*-dicyclohexylcarbodiimide (DCC), 4-(dimethylamino)pyridinium toluene-*p*-sulfonate (DPTS), 4-pyrrolidinopyridine (4-ppy), CH_2Cl_2, 0 °C and then room temperature, 20 h, 97%; (b) $Zn(BF_4)_2$, THF/H_2O, 50 °C, 72 h, 88%; (c) **5**, DCC, DPTS, 4-ppy, CH_2Cl_2, 0 °C and then room temperature, 24 h, 82%; (d) $Zn(BF_4)_2$, THF/H_2O, 60 °C, 24 h, 85%.

the determination of the absolute configuration of the newly formed stereogenic centers (in the pyrrolidine ring), see below.

The synthesis of the second-generation dendron is shown in Scheme 2. Esterification of **4** (see Scheme S1 in the Supporting Information for the synthesis) with O-protected 5-hydroxyisophthalic acid **5**[20] in the presence of *N,N′*-dicyclohexylcarbodiimide (DCC), 4-(dimethylamino)pyridinium toluene-*p*-sulfonate (DPTS), and 4-pyrrolidinopyridine (4-ppy) gave the first-generation dendron **6**, which was deprotected with $Zn(BF_4)_2$ to give **7**. Esterification of **5** with **7** led to the second-generation dendron **8**, the deprotection of which with $Zn(BF_4)_2$ gave the phenol derivative **9**.

Finally, the synthesis of diastereoisomeric fullerodendrimers is described in Scheme 3. Deprotection of the *tert*-butyl ester function of (*R,S*)-**1**, (*R,R*)-**1**, (*S,R*)-**1**, and (*S,S*)-**1** with trifluoracetic acid led to the corresponding carboxylic acid derivatives, which were condensed with the phenol-based dendron **9** in the presence of DCC and DPTS to give (*R,S*)-**2**, (*R,R*)-**2**, (*S,R*)-**2**, and (*S,S*)-**2**.

The structures and purities of the new compounds were confirmed by ^1H NMR spectroscopy and elemental analysis. The fullerene derivatives were also characterized by UV−vis and CD spectral analyses. The UV−vis spectra are in agreement with the fulleropyrrolidine structure[6] (illustrative examples are

Scheme 3[a]

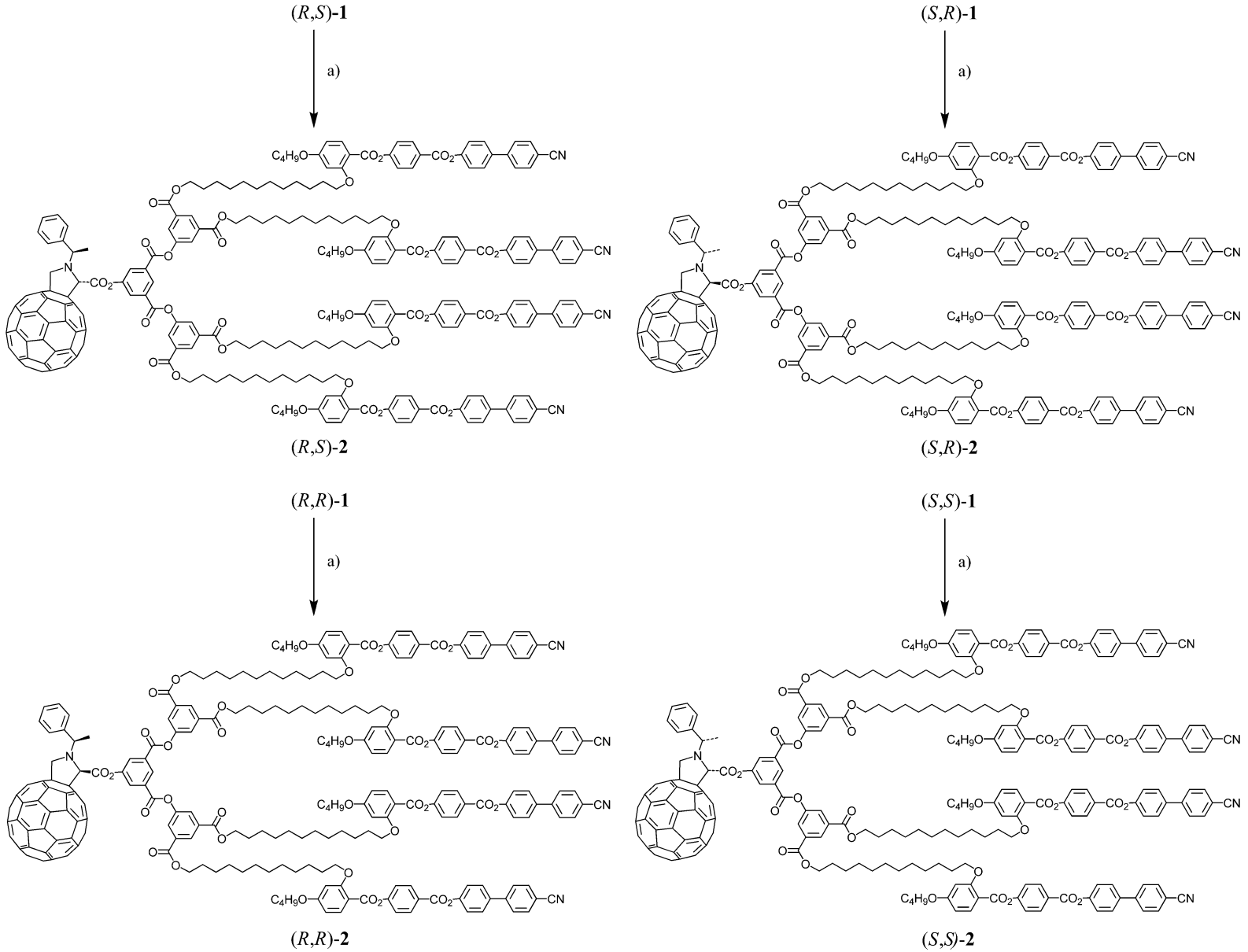

[a] Legend: (a) TFA, CH_2Cl_2, room temperature, 20 h and then **9**, DCC, DPTS, CH_2Cl_2, 0 °C and then room temperature, 4 h, 58% for (*R*,*S*)-**2**, 48% for (*R*,*R*)-**2**, 47% for (*S*,*R*)-**2**, 44% for (*S*,*S*)-**2**. For abbreviations, see the caption of Scheme 2.

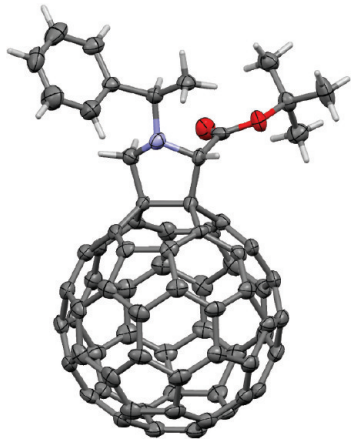

Figure 1. View of the molecular structure of the compound (*R*,*S*)-**1** with thermal ellipsoids drawn at the 50% probability level (the solvent molecule of toluene has been omitted for clarity).

shown in Figure S1 in the Supporting Information). Size exclusion chromatography (SEC) confirmed that monodisperse macromolecules were obtained (Table S1, Supporting Information).

Structure Determination. The slow diffusion of benzonitrile in a toluene solution containing the compound that eluted first on chromatography for the synthesis of (*R*,*S*)-**1**/(*R*,*R*)-**1**, i.e. from (*R*)-(+)-α-methylbenzylamine, gave dark red rodlike crystals which were analyzed by X-ray diffraction (Figure 1). The (*R*,*S*)-**1** derivative crystallized in the chiral orthorhombic space group $P2_12_12_1$ as a toluene solvate (see the Supporting Information).

Chiroptical Properties. The CD spectra of (*R*,*S*)-**1**, (*R*,*R*)-**1**, (*R*,*S*)-**2**, and (*R*,*R*)-**2** are shown in Figure 2 (for (*S*,*R*)-**1**, (*S*,*S*)-**1**, (*S*,*R*)-**2**, and (*S*,*S*)-**2**, see Figure S2 in the Supporting Information). They all display a strong Cotton effect at 430 nm, in agreement with the UV−vis spectra.[18,21] Prato et al. demonstrated that it is possible to correlate the sign of this CD peak with the absolute configuration of the asymmetric carbon atom of the pyrrolidine ring: i.e., a negative Cotton effect at 430 nm corresponds to the *S* configuration, whereas a positive Cotton effect corresponds to the *R* configuration.[18] This behavior was confirmed with (*R*,*S*)-**1**, for which the absolute configuration of the asymmetric carbon atom was determined by X-ray diffraction (see above). Indeed, on the basis of studies by Prato's group,[18] this compound should display a negative Cotton effect at 430 nm, which is actually the case. From the results obtained for (*R*,*S*)-**1**, the stereochemistry of the other diastereoisomers can be unambiguously established.

NMR Spectroscopy. The full and unequivocal attribution of all ^{1}H and ^{13}C resonances of the four diastereoisomers **1** dissolved in $CDCl_3$ was performed using standard 1D and 2D NMR experiments. The diastereoisomeric signatures can be easily confirmed. Indeed, comparison of the ^{1}H NMR spectra of (*S*,*S*)-**1** (part A of Figure 3) and (*S*,*R*)-**1** (part B of Figure 3) shows different chemical shifts for the protons of the pyrrolidine ring. The doublets (one for each H of the CH_2 group of the pyrrolidine) resonate at δ 5.10 and 4.39 ppm for (*S*,*R*)-**1** and at δ 5.33 and 4.72 ppm for (*S*,*S*)-**1**. The proton H_1 of the

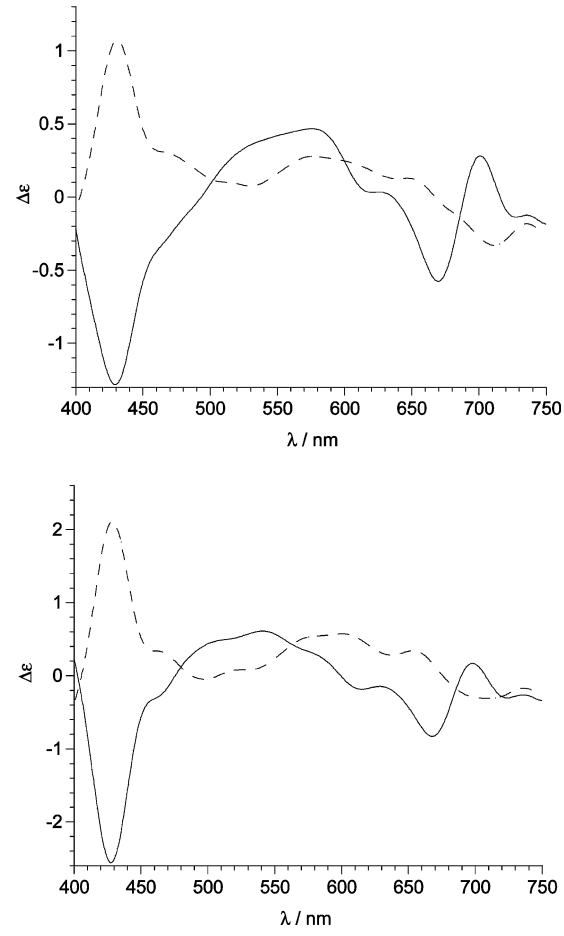

Figure 2. CD spectra of (top) (*R*,*R*)-**1** (dotted line) and (*R*,*S*)-**1** (solid line) and of (bottom) (*R*,*R*)-**2** (dotted line) and (*R*,*S*)-**2** (solid line) in CH_2Cl_2.

asymmetric center on the pyrrolidine resonates as a singlet at δ 5.62 and 4.87 ppm for (*S*,*R*)-**1** and (*S*,*S*)-**1**, respectively. As expected, similar results were obtained for the other two diastereoisomers. The correct attribution of the diastereotopic protons H_2 and $H_{2'}$ was achieved using 1D ROESY experiments and on the basis of the structure obtained for (*R*,*S*)-**1** (Figure 1). Interestingly, the change of the configuration of the asymmetric carbon of the pyrrolidine ring from *R* to *S* has significant and specific effects on the ^{1}H chemical shifts, but only marginal effects on the ^{13}C chemical shifts. Not surprisingly, the configuration of this carbon has nearly no effect on the aromatic protons but induces a slight upfield shift (∼0.1−0.3 ppm) for H_2, H_2', and H_3 (Figure 3). The effect on the H_1 proton is more subtle to understand, as it resonates at 5.62 ppm for (*S*,*R*)-**1**, while it is downfield by 0.8 ppm in the case of (*S*,*S*)-**1**. To explain this difference, 1D ROESY experiments with selective excitation of the H_1 resonance were performed. For (*S*,*S*)-**1**, an intense ROE enhancement between H_1 and H_{ortho} and a weak ROE enhancement between H_1 and H_{meta} is observed, while for the (*S*,*R*)-**1** isomer only a weak ROE enhancement between H_1 and H_{ortho} is observed (Figure 4). This result indicates the spatial proximity between H_1 and the aromatic ring in (*S*,*S*)-**1**: it can be deduced from the simultaneous observation of ROE enhancements between H_1 and H_{ortho} and between H_1 and H_{meta} that H_1 lies in the shielding zone of the aromatic ring. This explains why H_1 in (*S*,*S*)-**1** is downfield by 0.8 ppm relative to H_1 in (*S*,*R*)-**1**.

(14) (a) Campidelli, S.; Eng, C.; Saez, I. M.; Goodby, J. W.; Deschenaux, R. *Chem. Commun.* **2003**, 1520. (b) Campidelli, S.; Brandmüller, T.; Hirsch, A.; Saez, I. M.; Goodby, J. W.; Deschenaux, R. *Chem. Commun.* **2006**, 4282.

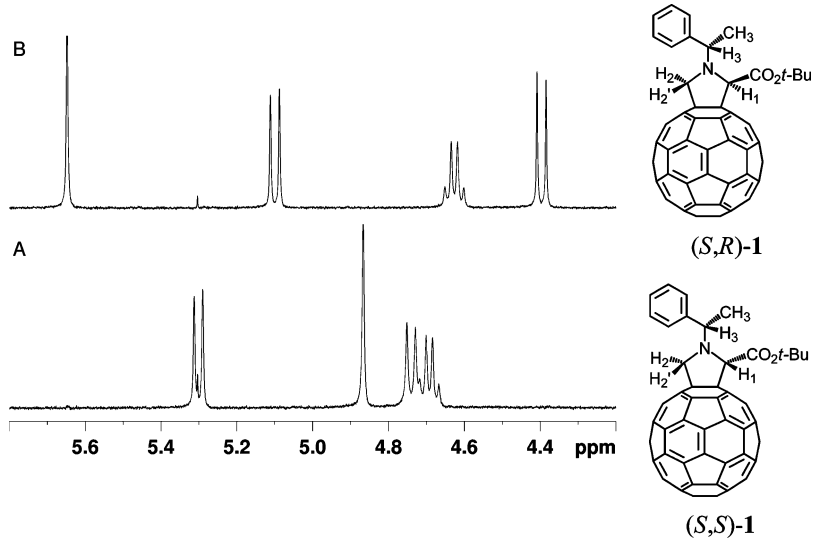

Figure 3. Expansions of the ^{1}H NMR spectra of (*S*,*S*)-**1** (A) and (*S*,*R*)-**1** (B) showing the protons of the pyrrolidine ring and the attribution. The molecular structures of the respective compounds are shown next to the spectra.

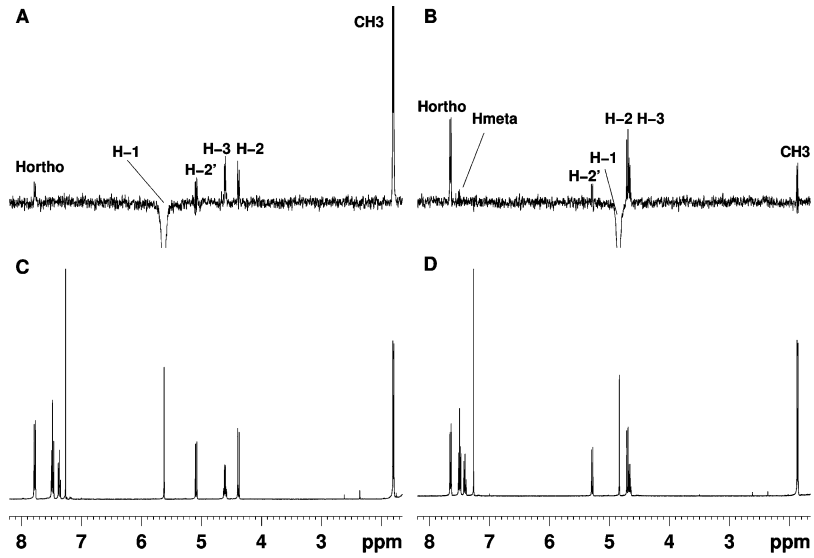

Figure 4. ^{1}H NMR spectra of (*S*,*R*)-**1** (C) and (*S*,*S*)-**1** (D) and the corresponding 1D ^{1}H selective ROESY spectra of (*S*,*R*)-**1** (A) and (*S*,*S*)-**1** (B) after H-1 was selectively excited. The protons H-1 are phased negatively such as ROE enhancements show positive signals.

Liquid-Crystalline Properties. The mesomorphic and thermal properties of the liquid-crystalline materials were investigated by polarized optical microscopy (POM) and differential scanning calorimetry (DSC). The phase-transition temperatures and enthalpy changes are reported in Table 1. The nonchiral intermediates **4** and **6**−**9** exhibit the N phase, which was identified by POM from the formation of *schlieren* and homeotropic textures. The phenol derivatives give higher clearing points than the corresponding O-protected precursors (compare **6** with **7** and **8** with **9**). This behavior is, most likely, due to stronger intermolecular interactions because of the HO groups that induce hydrogen bonding. Due to the limited thermal stability of the phenol derivatives, their transition temperatures are only indicative. As for the optically active fullerodendrimers (*R*,*S*)-**2**, (*R*,*R*)-**2**, (*S*,*R*)-**2**, and (*S*,*S*)-**2**, they all display the N* phase. The clearing points of the fullerodendrimers are lower than those of the phenol precursors. This result is an indication that C_{60} destabilizes the mesophases, possibly as a consequence of its large molecular volume (about 700 Å^3).

Table 1. Phase-Transition Temperatures[a] and Enthalpy Changes of the Mesogenic Unit, Dendrons, and Fullerodendrimers

compd	T_g (°C)	transition	temp (°C)	ΔH (kJ mol^{-1})
4	1	N → I	166	0.76
6	12	N → I	116[b]	0.84
7	32	N → I	185	1.84
8	47	N → I	135	2.16
9	51	N → I	164	2.21
(*R*,*S*)-**2**	69	N* → I	109	0.94
(*R*,*R*)-**2**	68	N* → I	108	0.86
(*S*,*R*)-**2**	71	N* → I	106	0.23
(*S*,*S*)-**2**	74	N* → I	106	0.36

[a] Definitions: T_g, glass transition temperature; N, nematic phase; N*, chiral nematic phase; I = isotropic liquid. Temperatures are given as the onset of the peaks obtained during the second heating run; the T_g values were determined during the first cooling run. [b] Determined as the maximum of the peak obtained during the second heating run.

The samples were studied by POM on the pristine solids, on untreated glass slides, and between a coverslip and slide, heating

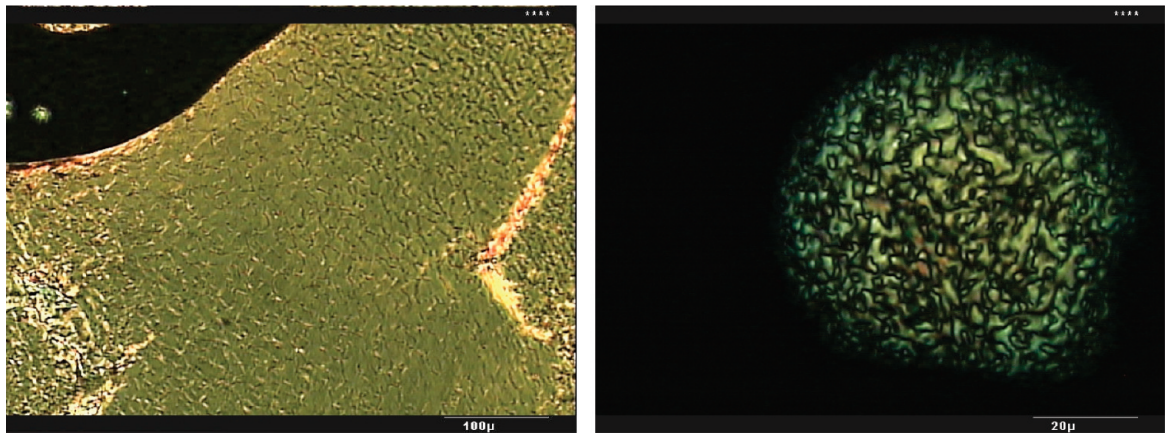

Figure 5. Grandjean-plane texture displayed by (*R*,*S*)-**2** (left) and pseudofocal conic texture displayed by (*R*,*R*)-**2** (right).

to the isotropic point and cooled at 0.2 °C min^{-1} to 108 °C, to give a grainy, birefringent orange-colored melt without specific characteristic textures or defects. However, upon annealing at this temperature, most of the areas of the preparation evolved to display the Grandjean plane texture with characteristic oily streak defects, which allows for the unequivocal assignment of the mesophase as chiral nematic (Figure 5). In some areas of the preparations, the planar anchoring of the Grandjean texture gradually became populated by the fingerprint defects arising from homeotropic boundary conditions, which corresponds to the helical pitch. However, it is interesting to note the contrast in behavior between the four isomers: for example, (*R*,*S*)-**2** and (*S*,*R*)-**2** develop characteristic natural textures on cooling from the isotropic liquid with more ease than (*R*,*R*)-**2** and (*S*,*S*)-**2**, which required longer periods of annealing and/or alignment layers to develop.

The cholesteric pitch was determined from the fingerprint texture (Figure 6), since the distance between adjacent, equidistant dark (or bright) lines corresponds to half of the pitch length.[22] The ρ values (Table 2) indicate that these materials have relatively long pitches (3−4 μm). The absolute values are comparable with the results obtained for other low molar mass derivatives of α-methylbenzylamine.[23] The handedness of the cholesteric helix was established from observations of the natural textures under polarized light, showing that the enantiomers in each pair have opposite twist directions (Table 2).

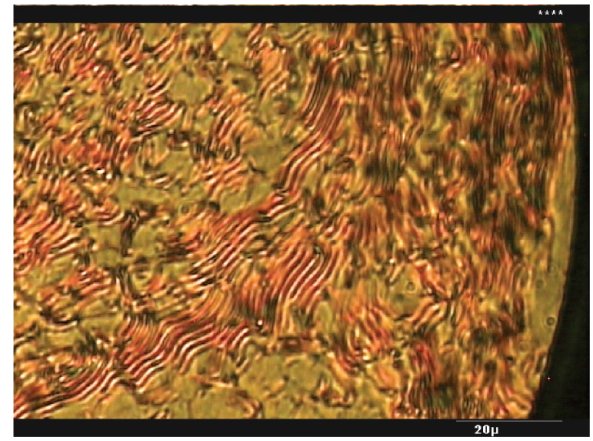

Figure 6. Fingerprint texture displayed by (*R*,*S*)-**2** at room temperature.

Table 2. Structural Characterization of the N* Phase Displayed by the Chiral Fullerodendrimers

	pitch ρ (μm) at 25 °C	handedness of the cholesteric helix
(*R*,*S*)-**2**	2.8 ± 0.02	right
(*R*,*R*)-**2**	3.0 ± 0.1	right
(*S*,*R*)-**2**	4.0 ± 0.2	left
(*S*,*S*)-**2**	4.1 ± 0.1	left

Furthermore, we observe that the configuration of the phenylamine carbon [Ph*C*H(CH_3)] seems to dominate the chiral response in the mesophase; the isomers with an *R* configuration at the phenylamine carbon produce a right-handed helix, whereas the *S* configuration at the phenylamine carbon induces a left-handed helix. However, these studies do not allow us to distinguish at the present what is the contribution of the chiral carbon at the pyrrolidine ring to the mesophase chirality.

Interestingly, the observation of the N* phase for (*R*,*S*)-**2**, (*R*,*R*)-**2**, (*S*,*R*)-**2**, and (*S*,*S*)-**2** is proof that the liquid-crystalline properties of those compounds arise from the combination of the structural characteristics of both molecular building blocks, i.e., the chiral C_{60} unit and the nematogenic dendron, thus allowing for the first time in this class of materials to establish the correlation between

(15) (a) Hawker, C.; Fréchet, J. M. J. *J. Chem. Soc., Chem. Commun.* **1990**, 1010. (b) Hawker, C. J.; Fréchet, J. M. J. *J. Am. Chem. Soc.* **1990**, *112*, 7638. (c) Grayson, S. M.; Fréchet, J. M. J. *Chem. Rev.* **2001**, *101*, 3819.
(16) (a) Peroukidis, S. D.; Vanakaras, A. G.; Photinos, D. J. *J. Chem. Phys.* **2005**, *123*, 164904. (b) Peroukidis, S. D.; Vanakaras, A. G.; Photinos, D. J. *J. Phys. Chem. B* **2008**, *112*, 12761.
(17) (a) Saez, I. M.; Goodby, J. W. *J. Mater. Chem.* **2005**, *15*, 26. (b) Goodby, J. W.; Saez, I. M.; Cowling, S. J.; Görtz, V.; Draper, M.; Hall, A. W.; Sia, S.; Cosquer, G.; Lee, S.-E.; Raynes, E. P. *Angew. Chem., Int. Ed.* **2008**, *47*, 2754.
(18) (a) Maggini, M.; Scorrano, G.; Bianco, A.; Toniolo, C.; Sijbesma, R. P.; Wudl, F.; Prato, M. *J. Chem. Soc., Chem. Commun.* **1994**, 305. (b) Bianco, A.; Maggini, M.; Scorrano, G.; Toniolo, C.; Marconi, G.; Villani, C.; Prato, M. *J. Am. Chem. Soc.* **1996**, *118*, 4072.
(19) (a) Illescas, B. M.; Martín, N.; Poater, J.; Solà, M.; Aguado, G. P.; Ortuño, R. M. *J. Org. Chem.* **2005**, *70*, 6929. (b) Filippone, S.; Maroto, E. E.; Martín-Domenech, Á.; Suarez, M.; Martín, N. *Nat. Chem.* **2009**, *1*, 578.
(20) Miller, T. M.; Kwock, E. W.; Neenan, T. X. *Macromolecules* **1992**, *25*, 3143.
(21) Wilson, S. R.; Wu, Y.; Kaprinidis, N. A.; Schuster, D. I.; Welch, C. J. *J. Org. Chem.* **1993**, *58*, 6548.
(22) (a) *Chirality in Liquid Crystals*, Kitzerow, H.-S., Bahr, C., Eds.; Springer-Verlag: New York, 2001. (b) Gottarelli, G.; Spada, G. P. In *Topics in Stereochemistry*; Green, M. M., Nolte, R. J. M., Meijer, E. W., Eds.; Wiley: New York, 2003, Materials Chirality, Vol. 24, p 425.

molecular and mesophase chirality. Chiral fullerenes can therefore be used as platforms for the design of optically active liquid crystals that display chiral mesophases.

Conclusions

The synthesis of liquid-crystalline, diastereoisomerically pure fullerodendrimers was successfully achieved. Four diastereoisomerically pure fulleropyrrolidines ((*R*,*S*)-**1**, (*R*,*R*)-**1**, (*S*,*R*)-**1**, and (*S*,*S*)-**1**) were connected to a second-generation dendron which displays the nematic (N) phase. The resulting fullerodendrimers ((*R*,*S*)-**2**, (*R*,*R*)-**2**, (*S*,*R*)-**2**, and (*S*,*S*)-**2**) exhibit the chiral nematic (N*) phase. The formation and nature of the latter mesophase arise from the combination of the chirality of the fulleropyrrolidine units with the nematogenic behavior of the dendritic liquid-crystalline promoter. Therefore, each subunit (i.e., the fulleropyrrolidine and the dendron) plays complementary roles to generate the desired mesophase in the final materials. Interestingly, other chiral mesophases may be obtained, such as the chiral smectic C (SmC*) phase, by selecting an appropriate dendron. Our study represents a new and general approach for the design of liquid-crystalline fullerenes, for which the chiroptical and liquid-crystalline properties can be tailored at the molecular level.

Acknowledgment. R.D. thanks the Swiss National Science Foundation (Grant No. 200020-119648) for financial support. We also acknowledge support from the European Science Foundation (ESF) under the EUROCORES SONS II - LCNANOP project.

Supporting Information Available: Text, figures, and tables giving techniques, experimental details, and analytical data of the new compounds and a CIF file giving crystallographic data for compound (*R*,*S*)-**1**. This material is available free of charge via the Internet at http://pubs.acs.org.

JA910128E

(23) (a) Semenkova, G. P.; Kutulya, L. A.; Shkolnikova, N. I.; Khandrimailova, T. V. *Cryst. Rep.* **2001**, *46*, 118. (b) Shkolnikova, N. I.; Kutulya, L. A.; Pivnenko, N. S.; Roshal, A. D.; Semenkova, G. P. *Liq. Cryst.* **2007**, *34*, 1193. (c) Solladié, G.; Zimmermann, R. G. *Angew. Chem., Int. Ed. Engl.* **1984**, *23*, 348.